Dual inhibition of SNARE complex formation by tomosyn ensures controlled neurotransmitter release

Toshiaki Sakisaka,[1] Yasunori Yamamoto,[1] Sumiko Mochida,[3] Michiko Nakamura,[4] Kouki Nishikawa,[5] Hiroyoshi Ishizaki,[6] Miki Okamoto-Tanaka,[6] Jun Miyoshi,[6] Yoshinori Fujiyoshi,[5] Toshiya Manabe,[4,7] and Yoshimi Takai[2]

[1]Division of Membrane Dynamics, Department of Physiology and Cell Biology, and [2]Division of Molecular and Cellular Biology, Department of Biochemistry and Molecular Biology, Kobe University Graduate School of Medicine, Kobe 650-0017, Japan
[3]Department of Physiology, Tokyo Medical University, Tokyo 160-8402, Japan
[4]Division of Neuronal Network, Department of Basic Medical Sciences, Institute of Medical Science, University of Tokyo, Tokyo 108-8639, Japan
[5]Department of Biophysics, Kyoto University Graduate School of Science, Kyoto 606-8502, Japan
[6]Department of Molecular Biology, Osaka Medical Center for Cancer and Cardiovascular Disease, Osaka 537-8511, Japan
[7]Core Research for Evolutional Science and Technology, Japan Science and Technology Agency, Kawaguchi 332-0012, Japan

Neurotransmitter release from presynaptic nerve terminals is regulated by soluble NSF attachment protein receptor (SNARE) complex–mediated synaptic vesicle fusion. Tomosyn inhibits SNARE complex formation and neurotransmitter release by sequestering syntaxin-1 through its C-terminal vesicle-associated membrane protein (VAMP)–like domain (VLD). However, in tomosyn-deficient mice, the SNARE complex formation is unexpectedly decreased. In this study, we demonstrate that the N-terminal WD-40 repeat domain of tomosyn catalyzes the oligomerization of the SNARE complex. Microinjection of the tomosyn N-terminal WD-40 repeat domain into neurons prevented stimulated acetylcholine release. Thus, tomosyn inhibits neurotransmitter release by catalyzing oligomerization of the SNARE complex through the N-terminal WD-40 repeat domain in addition to the inhibitory activity of the C-terminal VLD.

Introduction

Synaptic vesicles are transported to the presynaptic plasma membrane where Ca^{2+} channels are located. Depolarization induces Ca^{2+} influx into the cytosol of nerve terminals through the Ca^{2+} channels, and this Ca^{2+} influx initiates the fusion of the vesicles with the plasma membrane, finally leading to exocytosis of neurotransmitters (Südhof, 2000). Soluble SNAREs are essential for the synaptic vesicle exocytosis (Sutton et al., 1998; Weber et al., 1998; Weis and Scheller, 1998; Jahn and Südhof, 1999; Jahn and Scheller, 2006). Synaptic vesicles are endowed with vesicle-associated membrane protein 2 (VAMP-2) as a vesicular SNARE, whereas the presynaptic plasma membrane is endowed with syntaxin-1 and SNAP-25 as target SNAREs. VAMP-2 interacts with SNAP-25 and syntaxin-1 to form a stable SNARE complex (Trimble et al., 1988; Bennett et al., 1992; Söllner et al., 1993; Chen and Scheller, 2001). The formation of the SNARE complex brings synaptic vesicles and the plasma membrane into close apposition and provides the energy that drives the mixing of the two lipid bilayers (Weber et al., 1998; Chen et al., 1999).

Tomosyn is a syntaxin-1–binding protein that we originally identified previously (Fujita et al., 1998). Tomosyn contains a large N-terminal domain with a WD-40 repeat domain and a C-terminal domain homologous to VAMP-2. The large N-terminal region of tomosyn shares similarity to the *Drosophila melanogaster* tumor suppressor lethal giant larvae (Lgl), the mammalian homologues M-Lgl1 and M-Lgl2, and the yeast proteins Sro7p and Sro77p (Lehman et al., 1999; Wirtz-Peitz and Knoblich, 2006). A structural study of tomosyn indicated that the C-terminal VAMP-like domain (VLD) of tomosyn acts as a SNARE domain that competes with VAMP-2, leading to inhibition of the formation of the SNARE complex (Pobbati et al., 2004). We previously showed that tomosyn is directly phosphorylated by cAMP-dependent protein kinase (PKA) and

T. Sakisaka and Y. Yamamoto contributed equally to this paper.

Correspondence to Y. Takai: ytakai@med.kobe-u.ac.jp

Abbreviations used in this paper: Ab, antibody; CSM, crude synaptic membrane; EPSP, excitatory postsynaptic potential; ES, embryonic stem; Lgl, lethal giant larvae; LTP, long-term potentiation; MBP, maltose-binding protein; PPF, paired-pulse facilitation; SCG, superior cervical ganglion; VAMP, vesicle-associated membrane protein; VLD, VAMP-like domain.

The online version of this article contains supplemental material.

The Rockefeller University Press $30.00
J. Cell Biol. Vol. 183 No. 2 323–337
www.jcb.org/cgi/doi/10.1083/jcb.200805150

that this reduces its interaction with syntaxin-1 and enhances the formation of the SNARE complex (Baba et al., 2005). In addition, Rho-associated serine/threonine kinase activated by Rho small G protein phosphorylates syntaxin-1, thereby increasing the affinity of syntaxin-1 for tomosyn and the formation of a stable complex between the two, resulting in inhibition of the formation of the SNARE complex during neurite extension (Sakisaka et al., 2004). Recent genetic studies in *Caenorhabditis elegans* showed that TOM-1, an orthologue of vertebrate tomosyn, inhibits the priming of synaptic vesicles and that this priming is modulated by the balance between TOM-1 and UNC-13 (Gracheva et al., 2006; McEwen et al., 2006). The large N-terminal WD-40 repeat domain of tomosyn was shown to be involved in the inhibitory role of tomosyn on exocytosis of dense core granules in adrenal chromaffin and PC12 cells (Constable et al., 2005; Yizhar et al., 2007). Thus, evidence is accumulating that tomosyn acts as a negative regulator for the formation of the SNARE complex, thereby inhibiting various vesicle fusion events. However, the precise molecular mechanism underlying the inhibitory action of the large N-terminal WD-40 repeat domain of tomosyn has yet to be elucidated.

In this study, we show that tomosyn catalyzes oligomerization of the SNARE complex upon the direct interactions of the WD-40 repeat domain with SNAP-25 and syntaxin-1. Tomosyn inhibits SNARE-dependent synaptic vesicle fusion via both N-terminal WD-40 repeat domain–mediated oligomerization of the SNARE complex and C-terminal VLD-based competitive inhibition of SNARE complex formation, resulting in potent inhibition of neurotransmitter release.

Results

Generation of tomosyn-deficient mice

To disrupt tomosyn in embryonic stem (ES) cells, gene targeting was used to replace the first coding exon and the 5′ half of exon 2 with an MC1-neomycin resistance cassette (Fig. 1 A). The targeting vector was electroporated into RW4 ES cells, and six G418-resistant colonies heterozygous for the tomosyn gene were selected. Cells from two independent ES clones were used to generate chimeric mice and successfully contributed to germline transmission. Tomosyn heterozygotes were intercrossed to produce homozygous mutant offspring (Fig. 1 B). Mice homozygous for the disrupted allele expressed no intact tomosyn protein as analyzed by immunoblotting (Fig. 1 C). The homozygous mice were born at a lower than expected frequency, but born homozygous mice appeared healthy. However, when we attempted to generate C57B/6 backcrossed homozygous mice, homozygous mice backcrossed for more than three generations were not born, possibly because of a low fertilization rate in C57B/6 heterozygous mice (unpublished data). In this study, we used hybrid mice between C57B/6 and BDF1 mice because backcrossing to the C57B/6 genetic background had been unsuccessful. First, we examined the effect of tomosyn deficiency on the expression levels of SNARE proteins, including syntaxin-1, SNAP-25, VAMP-2, and complexin. No significant changes were observed as estimated by immunoblotting of the homogenates of P20 cerebra with antibodies (Abs) against the respective proteins. These results indicate that tomosyn deficiency does not affect the expression levels of SNARE proteins.

Enhanced synaptic transmission in tomosyn-deficient mice

We characterized the tomosyn-deficient mice electrophysiologically. First, we examined the efficacy of synaptic transmission at hippocampal mossy fiber synapses by measuring input–output relationships of excitatory postsynaptic potentials (EPSPs). EPSPs were increased in tomosyn-deficient mice at all stimulus intensities tested (Fig. 1 D), indicating that synaptic transmission was enhanced. Next, we examined presynaptic short-term plasticity by inducing paired-pulse facilitation (PPF) at mossy fiber synapses (Fig. 1 E). PPF of tomosyn-deficient mice was decreased at all interstimulus intervals tested, indicating that the probability of neurotransmitter release was increased in tomosyn-deficient mice. Finally, we examined long-term plasticity by inducing long-term potentiation (LTP; Fig. 1, F and G). The magnitude of mossy fiber LTP in tomosyn-deficient mice was reduced only during the first 20 min. The limitation of this reduction to the early stage of LTP in tomosyn-deficient mice may indicate that mossy fiber LTP consists of two phases, only the early one of which is regulated by tomosyn. Collectively, these results indicate that the probability of neurotransmitter release in tomosyn-deficient mice is higher than that in wild-type mice, suggesting that tomosyn inhibits synaptic vesicle fusion in vivo.

Reduced formation of the oligomerized SNARE complex in the tomosyn-deficient brain

Because the tomosyn deficiency facilitated synaptic transmission, we examined whether the formation of the SNARE complex was affected by tomosyn deficiency. For this purpose, we took advantage of the fact that the assembled SNARE complex is resistant to an SDS sample buffer at RT (Hayashi et al., 1994). Brain lysates from tomosyn-deficient and wild-type mice were solubilized in the SDS sample buffer and subjected to SDS-PAGE followed by immunoblotting with anti–syntaxin-1 and anti–SNAP-25 mAbs. Because tomosyn was known to inhibit the formation of the SNARE complex by competing with VAMP-2 (Fujita et al., 1998; Pobbati et al., 2004), we expected that the formation of the SNARE complex would be increased in tomosyn-deficient mice. Unexpectedly, the amount of the assembled SNARE complex in tomosyn-deficient mice was reduced compared with wild-type mice (Fig. 2 A). The molecular mass of the immunoblot band was apparently larger (~110 kD) than that of the expected single ternary SNARE complex (~50 kD). Because a previous study has suggested that the single ternary SNARE complex can form an oligomeric structure and exists as a star-shaped particle with three to four bundles in vivo (Rickman et al., 2005), we assumed that the higher molecular mass bands might represent an oligomerized SNARE complex. Glycerol density gradient ultracentrifugation confirmed that the higher molecular mass bands sedimented in fractions with the mass of the

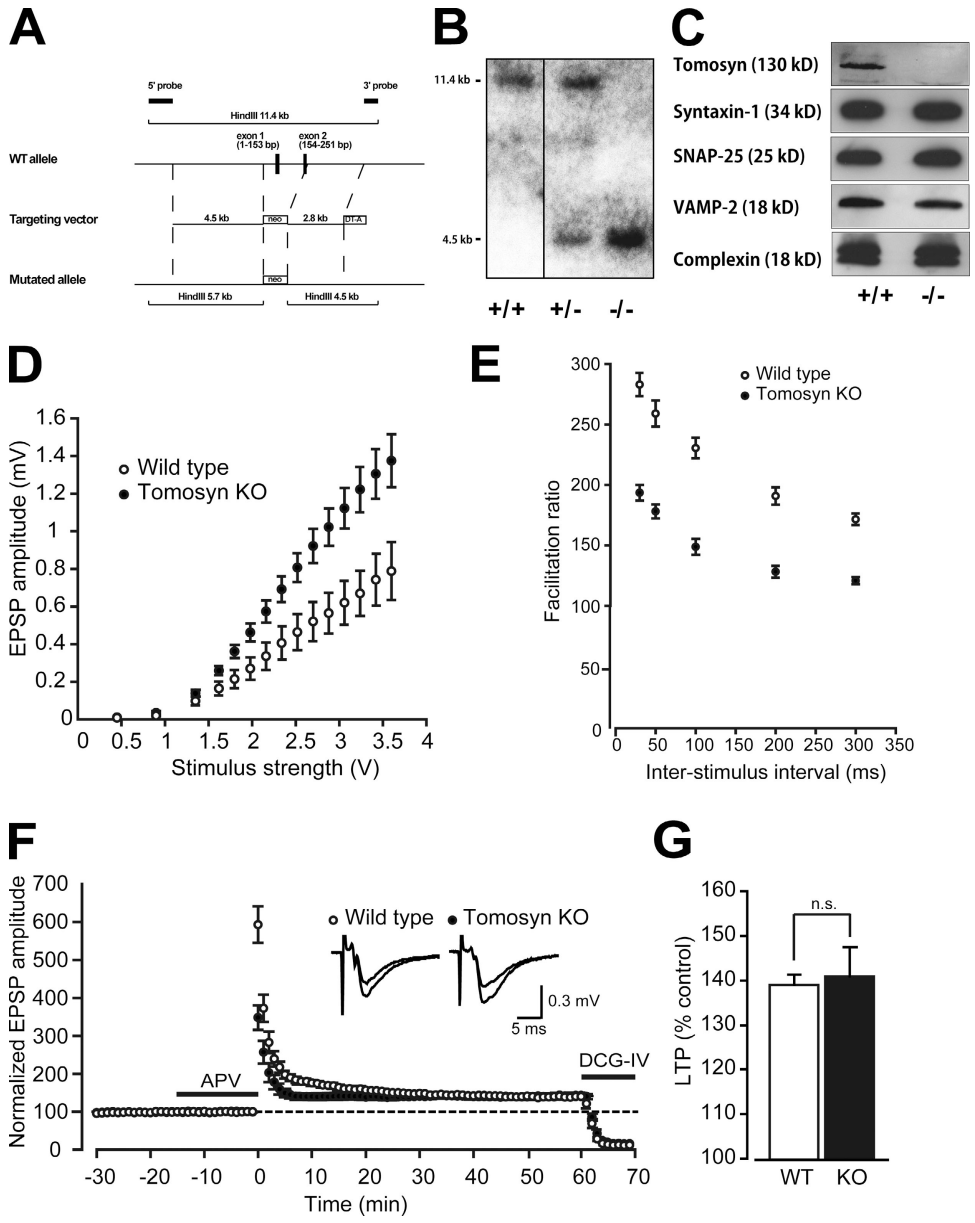

Figure 1. **Properties of synaptic transmission and plasticity at hippocampal mossy fiber synapses in tomosyn-deficient mice.** (A) Targeted disruption of the tomosyn gene. A targeting vector was designed to remove the genomic DNA segment of exon 1, its upstream intron, and the 5′ half of exon 2. The construct contained 4.5-kb 5′-flanking DNA sequences and 2.8-kb 3′-flanking DNA sequences. The diphtheria toxin DT-A cassette was inserted at the 3′ end. In the targeted allele, the MC1-neo cassette replaces 1.1 kb of genomic DNA. Homologous recombination was verified by using informative restriction fragments and diagnostic probes as indicated. (B) Southern hybridization using HindIII-digested DNA extracted from mouse tails and the 3′ external probe shown in A. (C) Immunoblot analysis of the SNARE proteins extracted from the brains of wild-type or tomosyn-deficient mice. (D) Input–output relationship of the EPSPs in wild-type (n = 11) and tomosyn-deficient mice (n = 11). (E) PPF induced by paired-pulse stimulation at various interstimulus intervals in wild-type (n = 10) and tomosyn-deficient mice (n = 10). (F) The averaged time course of LTP in wild-type and tomosyn-deficient mice. Tetanic stimulation (100 Hz for 1 s) was applied at 0 min in the presence of 50 μM D-APV (D-2-amino-5-phosphovaleric acid). After the LTP experiment, 1 μM DCG-IV (2S,2′R,3′R)-2-(2′,3′-dicarboxycyclopropyl)glycine), a group II metabotropic glutamate receptor agonist, was routinely applied to confirm that the recorded EPSP originated mostly at the mossy fiber synapses. If the amplitude of the residual EPSP was >15% of that of the original EPSP, the data were discarded. The dashed line indicates the normalized baseline excitatory postsynaptic potentials amplitude before tetanic stimulation. (G) Summary of LTP calculated as the percent increase in mean EPSP amplitude from 50–60 min after tetanic stimulation in wild-type and tomosyn-deficient mice. KO, knockout; n.s., not significant; WT, wild type. (D–G) Error bars represent SEM.

oligomerized SNARE complex (Fig. 2 B). Furthermore, the oligomerized SNARE complex was restored by the addition of recombinant maltose-binding protein (MBP)–tomosyn to brain extracts from tomosyn-deficient mice (Fig. 2 A, top). These results indicate that tomosyn enhances the oligomerization of the SNARE complex.

We next examined whether the tomosyn deficiency affected the cellular localization of SNARE proteins. We immunostained the hippocampi of adult wild-type and tomosyn-deficient mice with anti–SNAP-25 mAb (SMI81), which is highly specific for SNAP-25 and recognizes the SNAP-25 molecule incorporated into the SNARE complex (Hu et al., 2002; Rickman et al., 2005).

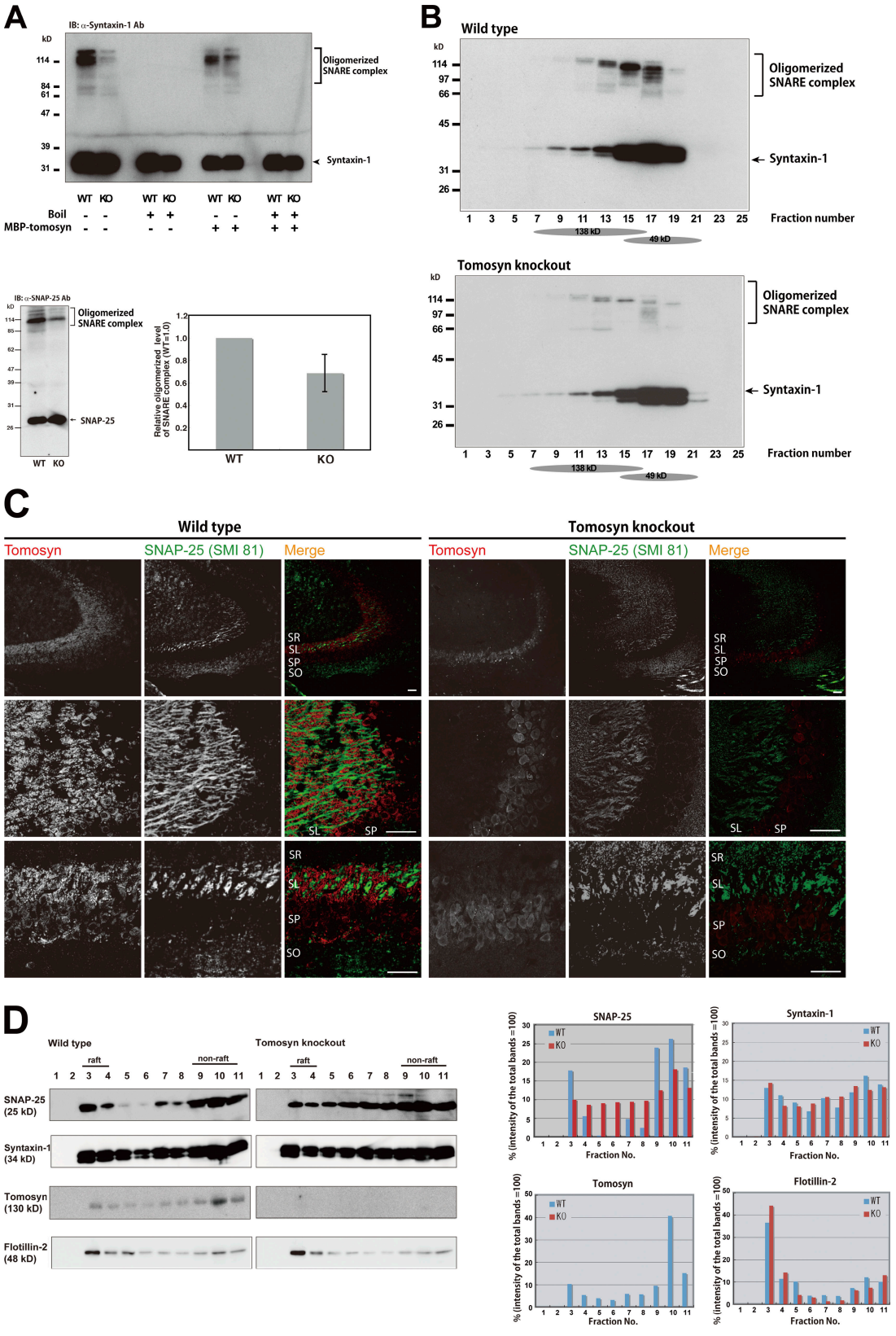

Figure 2. **Tomosyn-enhanced oligomerization of the SNARE complex in vivo.** (A) Immunoblot analysis of the oligomerized SNARE complex from the brains of wild-type or tomosyn-deficient mice. Extracts of brains from wild-type and tomosyn-deficient mice were incubated with or without MBP-tomosyn for 16 h. Each sample was solubilized in the SDS sample buffer at RT or with boiling and subjected to SDS-PAGE followed by immunoblotting. Top, immunoblotting with anti–syntaxin-1 mAb; bottom, immunoblotting with anti–SNAP-25 mAb. Quantification of the relative oligomerization of the SNARE complex is shown in the right panel. KO, knockout; WT, wild type. Error bar represents SD. (B) Glycerol density gradient ultracentrifugation of brain extracts from wild-type and tomosyn-deficient mice. Extracts from wild-type and tomosyn-deficient mice were subjected to 10–40% glycerol density gradient ultracentrifugation.

The immunoreactivity for SNAP-25 was prominently reduced in the tomosyn-deficient brain in comparison with the wild-type brain (Fig. 2 C). The most intense immunoreactivity for tomosyn was observed at the stratum lucidum of the CA3 area of the hippocampus in the wild-type brain, where the synapses between the mossy fiber terminals and dendrites of pyramidal cells localize. Immunoreactivity for SNAP-25 was also observed at the stratum lucidum of the CA3 area in the wild-type brain. Only faint colocalization of SNAP-25 with tomosyn was observed there. We further assessed the localization of the SNARE proteins biochemically. Recent studies have revealed that a subpopulation of SNAP-25 associates with lipid raft microdomains (Salaün et al., 2005; Puri and Roche, 2006). In wild-type mice, SNAP-25 was concentrated in both raft and nonraft fractions (Fig. 2 D), consistent with the previous studies (Salaün et al., 2005; Puri and Roche, 2006). However, tomosyn was predominantly detected in the nonraft fractions. This distinct distribution supports the faint colocalization of SNAP-25 with tomosyn on the immunostained brain sections. In tomosyn-deficient mice, the concentrations of SNAP-25 in raft and nonraft fractions were weakened, and SNAP-25 was diffusely distributed throughout all fractions. The distribution of syntaxin-1 was not affected by tomosyn deficiency. These results suggest that tomosyn regulates the concentration of SNAP-25 in lipid raft microdomains. The decreased immunostaining intensity for SNAP-25 is explained by the decreased formation of the oligomerized SNARE complex and the diffuse localization of SNAP-25 on the synaptic membrane in tomosyn-deficient mice.

Tomosyn-enhanced oligomerization of the SNARE complex in vitro

Next, we examined the ability of tomosyn to either enhance the formation of the SNARE complex or the oligomerization of the SNARE complex in a cell-free assay system using recombinant proteins. Recombinant MBP-tomosyn was incubated with syntaxin-1 lacking the transmembrane domain (referred to as syntaxin-1 hereafter), SNAP-25, and VAMP-2 lacking the transmembrane (referred to as VAMP-2 hereafter) for 12 h under reducing conditions. The reaction was terminated by the addition of the SDS sample buffer at RT, and each sample was subjected to SDS-PAGE followed by immunoblotting. The recombinant tomosyn protein shifted a 50-kD immunoreactive band to molecular masses of 90 and 130 kD in a dose-dependent manner (Fig. 3 A), suggesting that tomosyn enhanced the oligomerization of the SNARE complex. An intense band for MBP-tomosyn was detected at a higher molecular mass than the oligomerized SNARE complex, indicating that tomosyn was not incorporated into the SDS-resistant oligomerized SNARE complex. Characterization of the proteins extracted from the 130-kD band suggestive of the oligomerized SNARE complex and the 50-kD band suggestive of the monomeric SNARE complex revealed that both bands were composed of syntaxin-1, SNAP-25, and VAMP-2 at a ratio of 1:1:1, suggesting that the high molecular weight reaction product represents the oligomerized SNARE complex (Fig. S1, available at http://www.jcb.org/cgi/content/full/jcb.200805150/DC1).

Glycerol density gradient ultracentrifugation showed that the higher molecular mass bands observed after tomosyn treatment sedimented as expected for a higher order SNARE complex (Fig. 3 B). The complexes generated by tomosyn migrated further than the monomeric SNARE complex, confirming that the oligomerized SNARE complexes are larger than the monomeric SNARE complex. The SNARE complexes can be visualized by rotary shadowing electron microscopy as reported previously (Hohl et al., 1998; Rickman et al., 2005). The oligomerized SNARE complexes in fraction 11 were observed as star-shaped assemblies, whereas the monomeric SNARE complexes in fraction 17 appeared as rodlike structures (Fig. 3 C). We quantified the number of rods in the isolated oligomerized SNARE complexes. The particles bearing between two and four rods were observed in nearly 90% of total particles (Fig. 3 C). Collectively, these results indicate that tomosyn has an ability to enhance oligomerization of the SNARE complex in vitro.

Requirement of the intact configuration of SNAP-25 for the tomosyn action

It is well known that the SNARE complex is artificially cross-linked in vitro by oxidation of free cysteines on the hinge region of SNAP-25. Indeed, it was reported that the SNARE complex oligomer induced by complexin, which was originally reported by Tokumaru et al. (2001), was an oxidative artifact (Pabst et al., 2002). To avoid this artificial oxidation, we reacted the SNARE proteins and tomosyn under reducing conditions (1 mM DTT) in all in vitro assays, and reaction products were solubilized with the SDS sample buffer supplemented with a high concentration of a reducing reagent (75 mM DTT) before SDS-PAGE analysis. In addition, we reacted the SNARE proteins and tomosyn in the presence of TCEP (tris(2-carboxyethyl)phosphine), a stable reducing reagent, as described previously (Dai et al., 2007). Tomosyn enhanced the oligomerization of the SNARE complex even in the presence of 0.5 mM TCEP (Fig. S2 A, available at http://www.jcb.org/cgi/content/full/jcb.200805150/DC1), suggesting that the oligomerization of the SNARE complex was not simply caused by artificial oxidation. Next, we compared the activity of tomosyn to enhance the oligomerization of the SNARE complex with that of complexin. Consistent with a previous study (Pabst et al., 2002), complexin did not enhance the oligomerization of the SNARE complex under reducing conditions (Fig. S2 B). In contrast, tomosyn enhanced the oligomerization of the SNARE complex in a

An aliquot of each fraction was solubilized in the SDS sample buffer at RT and subjected to SDS-PAGE followed by immunoblotting with anti–syntaxin-1 mAb. (C) Localization of SNAP-25 in the hippocampal CA3 region in wild-type and tomosyn-deficient mice. Adult mouse hippocampal sections were doubly stained with antitomosyn pAb and anti–SNAP-25 (SMI81) mAb. The results shown are representative of three independent experiments. SL, stratum lucidum; SO, stratum oriens; SP, stratum pyramidale; SR, stratum radiatum. Bars, 30 µm. (D) Localization of the SNARE proteins in the lipid raft fraction. The CSM fractions from wild-type and tomosyn-deficient mice were solubilized with Lubrol WX, and the lipid raft–enriched fractions were separated by sucrose gradient centrifugation as described previously (Vetrivel et al., 2004). Each fraction was boiled in the SDS sample buffer and subjected to SDS-PAGE followed by immunoblotting. Flotillin-2 was used as a lipid raft marker. Quantification of the amount of protein in each fraction is shown in the right panel.

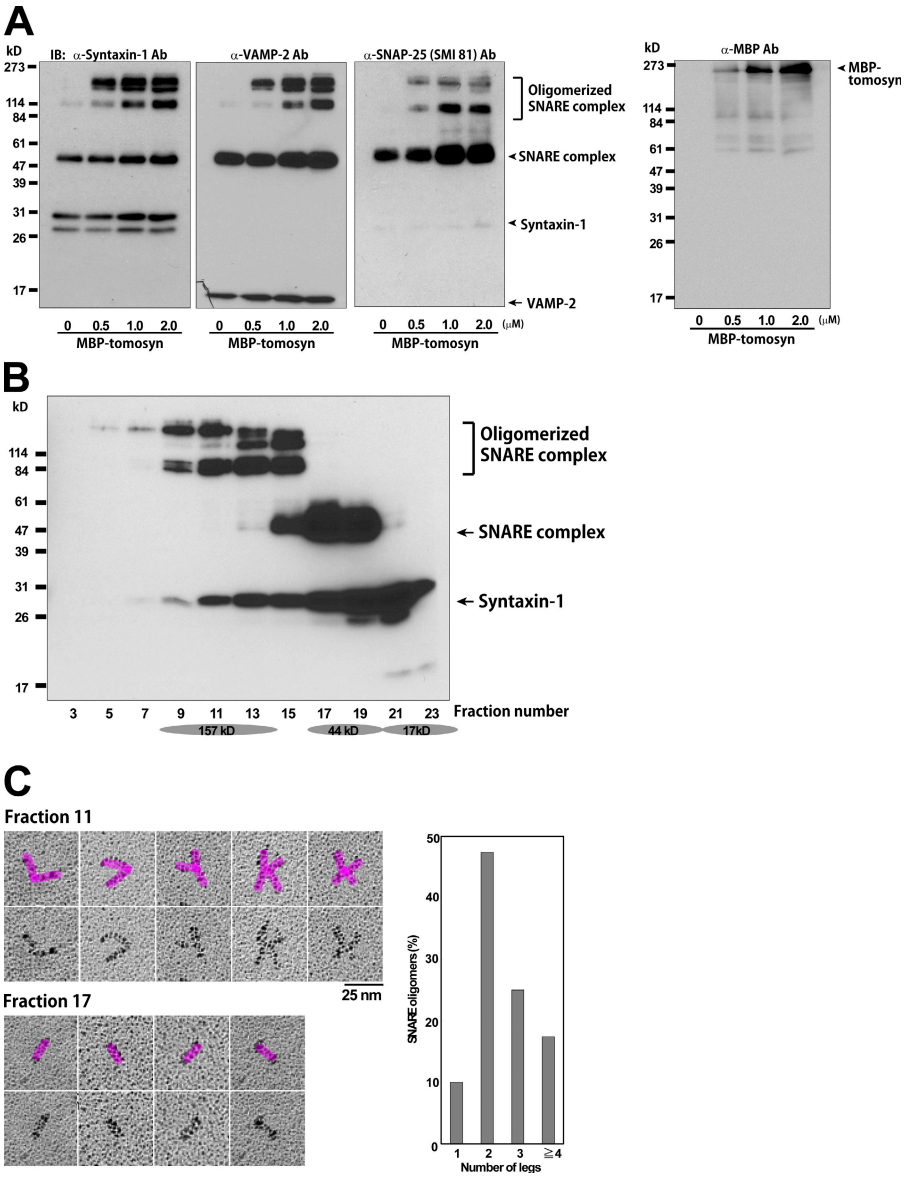

Figure 3. **Tomosyn-enhanced oligomerization of the SNARE complex in vitro.** (A) Reconstitution of tomosyn-induced oligomerization of the SNARE complex. Syntaxin-1, SNAP-25, and VAMP-2 were incubated in the presence or absence of the indicated amounts of MBP-tomosyn for 12 h under reducing conditions (1 mM DTT). The proteins were solubilized in the SDS sample buffer at RT and subjected to SDS-PAGE followed by immunoblotting with anti–syntaxin-1, anti–VAMP-2, or anti–SNAP-25 mAbs or anti-MBP pAb. (B) Analysis of molecular mass of the oligomerized SNARE complex by density gradient ultracentrifugation. Syntaxin-1, SNAP-25, and VAMP-2 were incubated in the presence of MBP-tomosyn for 12 h. The sample was subjected to a 10–30% glycerol density gradient. Aliquots of each gradient fraction were solubilized in the SDS sample buffer at RT and subjected to SDS-PAGE followed by immunoblotting with anti–syntaxin-1 mAb. (C) Morphology of the oligomerized SNARE complex. Rotary shadowing electron micrographs of the SNARE complexes recovered in gradient fractions 11 and 17. Quantification of the number of legs in the SNARE complex is shown in the right panel. The results shown are representative of three independent experiments.

dose-dependent manner. Furthermore, we reacted the N-terminal portion of SNAP-25 (residues 1–95), the C-terminal portion of SNAP-25 encompassing the cysteine-rich hinge region (residues 96–206), syntaxin-1, and VAMP-2 under reducing conditions in the presence of various amounts of MBP-tomosyn. The high molecular weight SNARE complexes indicative of the oligomerized SNARE complex were not formed in these reactions with divided SNAP-25 molecules (Fig. S2 C). These results indicate that the tomosyn-enhanced oligomerization of the SNARE complexes is not an artifact caused by oxidative cross-linking of SNAP-25 and that the intact structure of SNAP-25 is essential for the oligomerization of the SNARE complex.

Different affinities for SNAP-25 and syntaxin-1 between the N-terminal WD-40 repeat domain and the C-terminal VLD

Tomosyn has at least two domains: an N-terminal WD-40 repeat domain and a C-terminal VLD (Fujita et al., 1998). It has been shown that the VLD binds syntaxin-1 in the same manner as the SNARE domain and thereby competes with VAMP-2 in the formation of the SNARE complex (Pobbati et al., 2004). However, this competing activity of the VLD does not explain the activity of tomosyn to enhance the oligomerization of the SNARE complex. Therefore, we further characterized the possible interaction of tomosyn with the SNARE proteins. We first made an MBP-fused VLD (MBP-VLD; Fig. 4 A) and examined the interaction between the MBP-VLD and SNARE proteins. Syntaxin-1 and SNAP-25 bound to MBP-VLD as previously reported (Fig. 4 B; Yokoyama et al., 1999). VAMP-2 did not bind to MBP-VLD. Syntaxin-1 and SNAP-25 each enhanced the binding of the other to MBP-VLD by threefold, presumably reflecting the formation of a SNARE complex–like structure. VAMP-2 did not affect the binding of syntaxin-1 and SNAP-25 to MBP-VLD. We next made a VLD-deficient mutant of tomosyn (tomosyn-ΔVLD) as an MBP fusion protein and examined the interaction between MBP-tomosyn-ΔVLD and the SNARE proteins. Syntaxin-1 or SNAP-25 bound to MBP-tomosyn-ΔVLD (Fig. 4 C); however, VAMP-2 did not bind to MBP-tomosyn-ΔVLD.

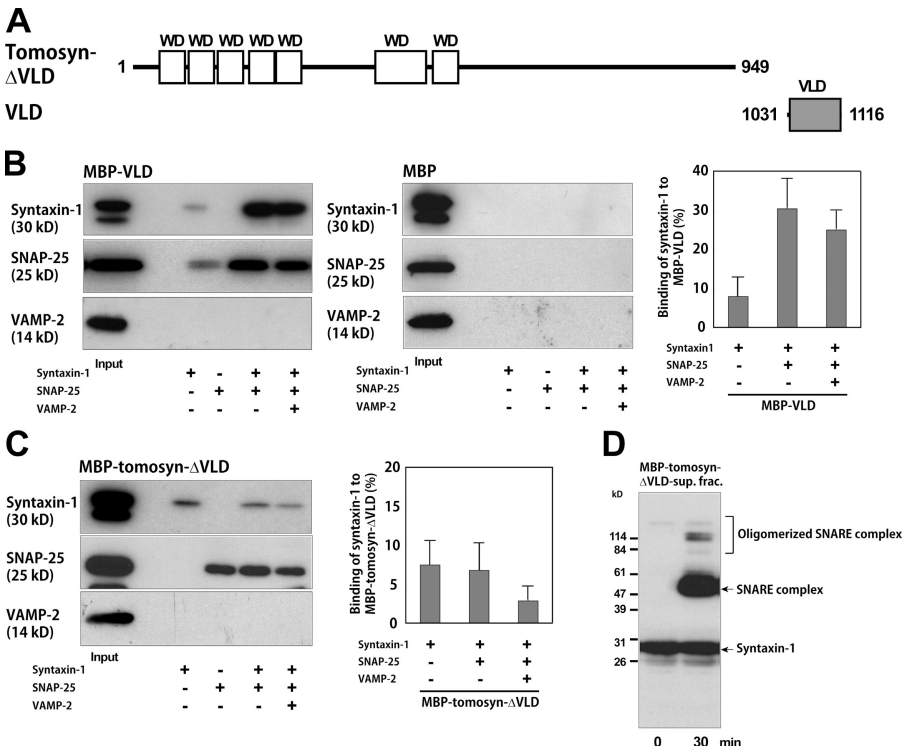

Figure 4. **Different affinities for SNAP-25 and syntaxin-1 between the N-terminal WD-40 repeat domain and the C-terminal VLD.** (A) Molecular structures of tomosyn-ΔVLD and VLD. (B) Binding of syntaxin-1 and SNAP-25 to the VLD of tomosyn. Quantification of the amount of syntaxin-1 bound to VLD is shown in the right panel. No binding of syntaxin-1 and SNAP-25 to MBP was shown in the middle panel (negative control). (C) Binding of syntaxin-1 and SNAP-25 to MBP-tomosyn-ΔVLD. Quantification of the amount of syntaxin-1 bound to MBP-tomosyn-ΔVLD is shown in the right panel. For B and C, syntaxin-1, SNAP-25, or the mixture of syntaxin-1 and SNAP-25 were incubated with the indicated MBP-fusion protein immobilized on amylose beads in the presence or absence of VAMP-2. After the beads were extensively washed, proteins bound to the beads were solubilized in the SDS sample buffer with boiling. The bound proteins were subjected to SDS-PAGE followed by immunoblotting with anti–syntaxin-1 mAb, anti–SNAP-25 mAb, or anti–VAMP-2 mAb. (B and C) Error bars represent SD. (D) Formation of the oligomerized SNARE complex in the supernatant fraction of the MBP-tomosyn-ΔVLD beads. Syntaxin-1, SNAP-25, and VAMP-2 were incubated with MBP-tomosyn-ΔVLD immobilized on amylose beads for the indicated periods of time. After centrifugation, the proteins in the supernatant fraction were solubilized in the SDS sample buffer at RT and subjected to SDS-PAGE followed by immunoblotting with anti–syntaxin-1 mAb.

Neither syntaxin-1 nor SNAP-25 enhanced the binding of the other to MBP-tomosyn-ΔVLD. VAMP-2 decreased the binding of syntaxin-1 and SNAP-25 to MBP-tomosyn-ΔVLD and induced the oligomerization of the SNARE complex (Fig. 4 D). These results indicate that the large N-terminal WD-40 repeat domain of tomosyn and the C-terminal VLD have different affinities for syntaxin-1 and SNAP-25.

Involvement of the N-terminal WD-40 repeat domain of tomosyn in the oligomerization of the SNARE complex

The aforementioned results prompted us to examine whether the N-terminal WD-40 repeat domain of tomosyn is involved in the enhanced oligomerization of the SNARE complex. We first preincubated full-length MBP-tomosyn or MBP-tomosyn-ΔVLD with syntaxin-1 and SNAP-25 under reducing conditions (Fig. 5 A) and added VAMP-2 to this mixture for 1 h. The reaction was terminated by addition of the SDS sample buffer at RT, and each sample was subjected to SDS-PAGE followed by immunoblotting with anti–syntaxin-1 mAb. Tomosyn-ΔVLD enhanced the oligomerization of the SNARE complex more potently than full-length MBP-tomosyn in a dose-dependent manner (Fig. 5 B). We next examined the kinetics of the tomosyn-induced oligomerization of the SNARE complex. We first preincubated full-length MBP-tomosyn or MBP-tomosyn-ΔVLD with syntaxin-1 and SNAP-25 under reducing conditions and added VAMP-2 to this mixture for the indicated periods of time. Tomosyn-ΔVLD enhanced the oligomerization of the SNARE complex more potently than full-length MBP-tomosyn in a time-dependent manner (Fig. 5 C). It was shown that the VLD interacts with syntaxin-1 in a manner competitive with VAMP-2, forms the tomosyn complex, and down-regulates the formation of the SNARE complex (Fujita et al., 1998; Yokoyama et al., 1999; Hatsuzawa et al., 2003; Pobbati et al., 2004; Sakisaka et al., 2004). Consistent with these studies, full-length MBP-tomosyn reduced the formation of the monomeric SNARE complex compared with tomosyn-ΔVLD at earlier time points (Fig. 5 D). These results indicate that the N-terminal WD-40 repeat domain of tomosyn is sufficient for the oligomerization of the SNARE complex and that the VLD is dispensable.

We used syntaxin-1 lacking the transmembrane domain (syntaxin-1–ΔTM) and VAMP-2 lacking the transmembrane domain (VAMP-2–ΔTM) for all of the aforementioned in vitro assays. Next, we tested whether tomosyn enhanced the oligomerization of SNARE complexes containing full-length syntaxin-1 and full-length VAMP-2. Full-length syntaxin-1, SNAP-25, and full-length VAMP-2 were incubated in the presence or absence of MBP-tomosyn-ΔVLD. Tomosyn-ΔVLD enhanced the oligomerization of SNARE complexes composed of full-length syntaxin-1, SNAP-25, and VAMP-2 (Fig. S3 A, available at http://www.jcb.org/cgi/content/full/jcb.200805150/DC1). Visualization of the samples by rotary shadowing electron microscopy indicated that tomosyn enhanced the formation of star-shaped assemblies of SNARE complexes (Fig. S3 B). We also observed that the reaction of full-length syntaxin-1, SNAP-25, and VAMP-2 predominantly led to formation of oligomerized SNARE complexes by themselves, whereas the reaction of syntaxin-1–ΔTM, full-length SNAP-25, and VAMP-2–ΔTM predominantly led to formation of the monomeric SNARE

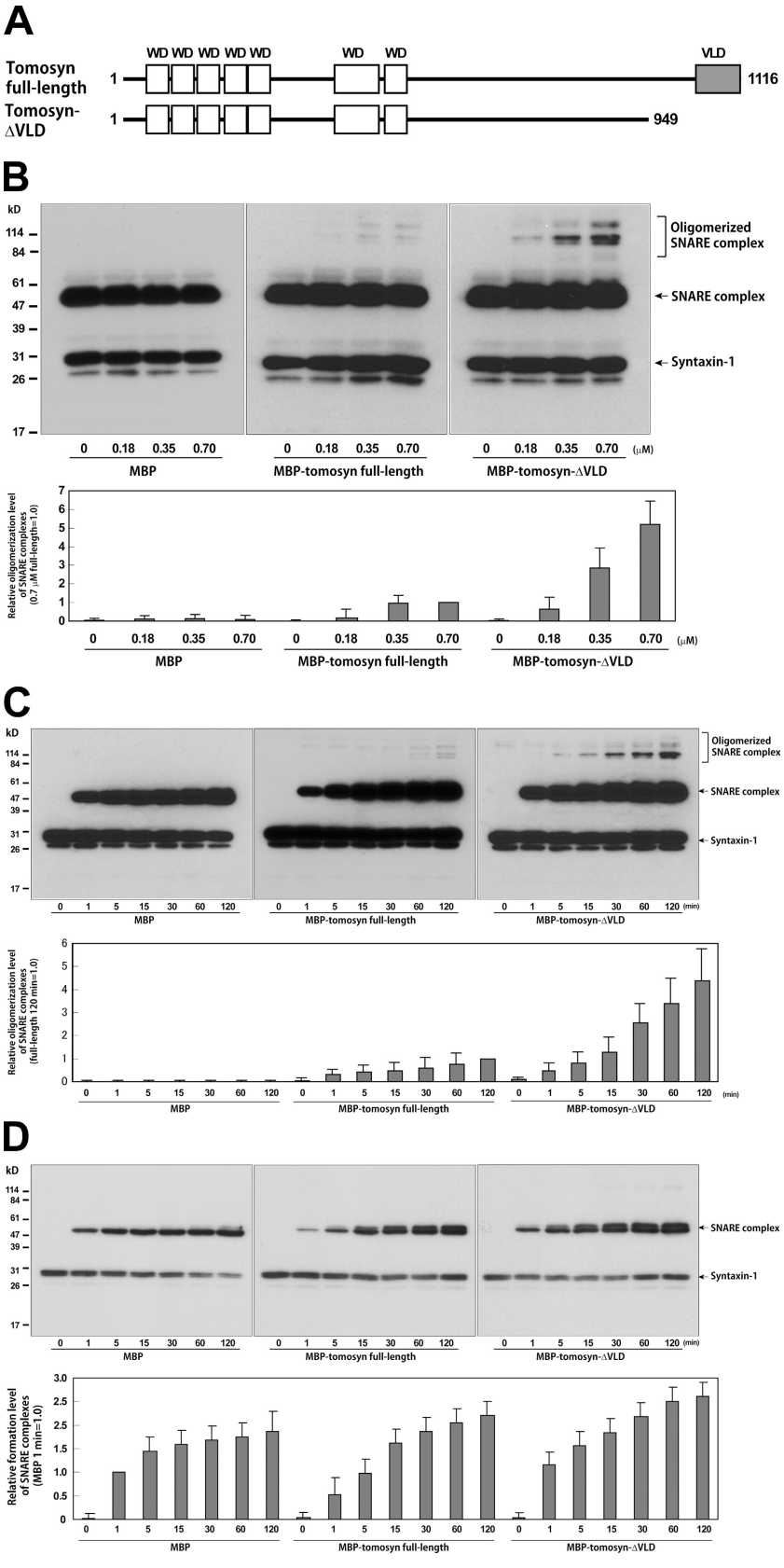

Figure 5. **Involvement of the N-terminal WD-40 repeat domain of tomosyn in the oligomerization of the SNARE complex.** (A) Molecular structures of tomosyn and tomosyn-ΔVLD. (B) Dose-dependent effect of tomosyn on the oligomerization of the SNARE complex. Syntaxin-1 and SNAP-25 were incubated in the presence of the indicated amounts of MBP-tomosyn or MBP-tomosyn-ΔVLD for 12 h. Each mixture was further incubated with VAMP-2 for 1 h. The proteins were solubilized in the SDS sample buffer at RT and subjected to SDS-PAGE followed by immunoblotting with anti–syntaxin-1 mAb. Quantification of the relative oligomerization of the SNARE complex is shown in the bottom panel. (C) Time-dependent effect of tomosyn on the oligomerization of the SNARE complex. Syntaxin-1 and SNAP-25 were incubated in the presence of MBP-tomosyn or MBP-tomosyn-ΔVLD for 12 h. Each mixture was further incubated with VAMP-2 for the indicated periods of time. The proteins were solubilized in the SDS sample buffer at RT and subjected to SDS-PAGE followed by immunoblotting with anti–syntaxin-1 mAb. Quantification of the relative oligomerization of the SNARE complex is shown in the bottom panel. (D) Difference in the formation of the ternary SNARE complex between MBP-tomosyn and MBP-tomosyn-ΔVLD. Short exposure of the film in C to detect the monomeric SNARE complex. Quantification of the relative formation of the ternary SNARE complex is shown in the bottom panel. The results shown are representative of three independent experiments. (B–D) Error bars represent SD.

complex (compare Fig. S1 A with Fig. S3 C, left). Characterization of the reaction products of full-length syntaxin-1, SNAP-25, and VAMP-2 showed that the oligomerized SNARE complex was composed of these molecules at a ratio of 1:1:1 (Fig. S3 C, right). Therefore, these results indicate that the transmembrane domains of syntaxin-1 and VAMP-2 have the ability to

facilitate the oligomerization of the SNARE complexes and that the WD-40 repeat domain of tomosyn enhances the oligomerization of the SNARE complex independently of the transmembrane domains of syntaxin-1 and VAMP-2. These results provide an explanation of our observation that the oligomerized SNARE complex, but not the monomeric complex, was detected in brain lysates from mouse brain (Fig. 2 A), although the monomeric SNARE complex was readily detected among the in vitro reaction products of syntaxin-1–ΔTM, full-length SNAP-25, and VAMP-2–ΔTM.

We further characterized the nature of the tomosyn-enhanced oligomerization of the SNARE complex. First, we titrated the SNARE proteins. Various amounts of the SNARE proteins were reacted in the absence or presence of MBP-tomosyn-ΔVLD (Fig. S4 A, available at http://www.jcb.org/cgi/content/full/jcb.200805150/DC1). The SNARE proteins formed the oligomerized SNARE complex in a dose-dependent manner, indicating that a higher amount of the monomeric SNARE complexes assembles as oligomers in a tomosyn-independent manner. The reactions in the presence of MBP-tomosyn-ΔVLD moderately enhanced the formation of the monomeric SNARE complex and dramatically enhanced the formation of the oligomerized SNARE complex at all concentrations of the SNARE proteins tested. Next, we examined whether tomosyn oligomerizes preassembled SNARE complexes. The SNARE proteins were fully reacted in advance, and the formed SNARE complexes (preassembled SNARE complexes) were reacted with MBP-tomosyn-ΔVLD (Fig. S4 B). MBP-tomosyn-ΔVLD enhanced oligomerization of the SNARE complex. Collectively, these results suggest that tomosyn achieves the oligomerization of the SNARE complex via both facilitation of the formation of the monomeric SNARE complex and enhancement of the oligomerization of the preassembled SNARE complex.

Regulation of N-terminal WD-40 repeat domain–induced oligomerization of the SNARE complex by the C-terminal VLD

We examined the effect of the VLD on large N-terminal WD-40 repeat domain–induced oligomerization of the SNARE complex. We first preincubated MBP-tomosyn-ΔVLD with syntaxin-1 and SNAP-25 in the presence of various amounts of MBP (control) or MBP-VLD (Fig. 6 A) and added VAMP-2 to this mixture for 1 h. The reaction was terminated by the addition of the SDS sample buffer at RT, and each sample was subjected to SDS-PAGE followed by immunoblotting with anti–syntaxin-1 mAb. MBP-VLD potently inhibited the formation of the ternary SNARE complex and the oligomerization of the SNARE complex in a dose-dependent manner (Fig. 6 B). Next, we examined the kinetics of the inhibitory effect of MBP-VLD on the N-terminal domain–induced oligomerization of the SNARE complex. MBP-VLD potently inhibited the formation of the ternary SNARE complex and the oligomerization of the SNARE complex in a time-dependent manner (Fig. 6 C). These results indicate that the C-terminal VLD of tomosyn inhibits the formation of the ternary SNARE complex and thereby suppresses the oligomerization of the SNARE complex, which was basally induced or enhanced by the large N-terminal WD-40 repeat domain of tomosyn. These results also suggest that although tomosyn negatively regulates formation of the ternary SNARE complex via the C-terminal VLD and positively regulates the oligomerization of the SNARE complex via the large N-terminal WD-40 repeat domain, the actions of the C-terminal VLD and the large N-terminal WD-40 repeat domain are mutually exclusive.

We previously reported that tomosyn is phosphorylated by PKA, leading to a decrease in its binding activity for VAMP-2 (Baba et al., 2005). Therefore, we examined whether the phosphorylation of tomosyn altered its activity to enhance the oligomerization of the SNARE complex. Syntaxin-1, SNAP-25, and VAMP-2 were reacted in the presence of either the PKA-phosphorylated form or nonphosphorylated form of tomosyn. The phosphorylated form of tomosyn enhanced the tomosyn-induced oligomerization of the SNARE complex more efficiently than the nonphosphorylated form (Fig. S5 A, available at http://www.jcb.org/cgi/content/full/jcb.200805150/DC1), suggesting that the activity of the WD-40 repeat domain to enhance the oligomerization of the SNARE complex is regulated by PKA-catalyzed phosphorylation.

Functional significance of the N-terminal WD-40 repeat domain of tomosyn for neurotransmitter release

To further confirm the functional significance of the N-terminal WD-40 repeat domain of tomosyn for neurotransmitter release, we used a synapse formed between superior cervical ganglion (SCG) neurons in culture (Ma and Mochida, 2007). First, we determined the precise binding site of tomosyn. The large N-terminal WD-40 repeat domain of tomosyn was divided into three fragments: fragment 1 (Frg. 1), which contained the first five WD-40 repeats, Frg. 2, which contained the second two WD-40 repeats, and Frg. 3, comprising the C-terminal region with no WD-40 repeats (Fig. 7 A). The fragments were expressed as MBP-fused proteins in *Escherichia coli*, immobilized on amylose resin, and reacted with the SNARE proteins. Frgs. 1 and 2, but not Frg. 3, bound syntaxin-1 (Fig. 7 B). Indeed, SNAP-25 bound the same WD-40 repeat domain encompassing Frgs. 1 and 2 as syntaxin-1 (Fig. S5 B). Next, we examined which domains were responsible for the oligomerization of the SNARE complex. Frgs. 1 and 2, but not Frg. 3, enhanced the oligomerization of the SNARE complex, in agreement with their affinity to syntaxin-1 (Fig. 7 C). These results indicate that the WD-40 repeat domains are responsible for the oligomerization of the SNARE complex. We injected the MBP-fused fragments of tomosyn into presynaptic cell bodies by microinjection and recorded EPSPs evoked by action potentials in the presynaptic neurons (Fig. 7, D–F). Injection of Frgs. 1 and 2 reduced EPSPs. In contrast, injection of Frg. 3 did not affect EPSPs. These results provide further evidence suggesting that tomosyn-enhanced oligomerization of the SNARE complex inhibits neurotransmitter release. Consistent with a previous study (Pobbati et al., 2004), we observed that the VLD inhibits the formation of the monomeric SNARE complex and that injection of the VLD into SCG neurons reduces EPSPs. VLD-injected neurons restored the reduced EPSPs faster than Frg. 1– and Frg. 2–injected neurons, indicating that Frgs. 1 and 2 inhibited neurotransmitter release more potently than the VLD. The sustained reduction of EPSPs in Frg. 1– and

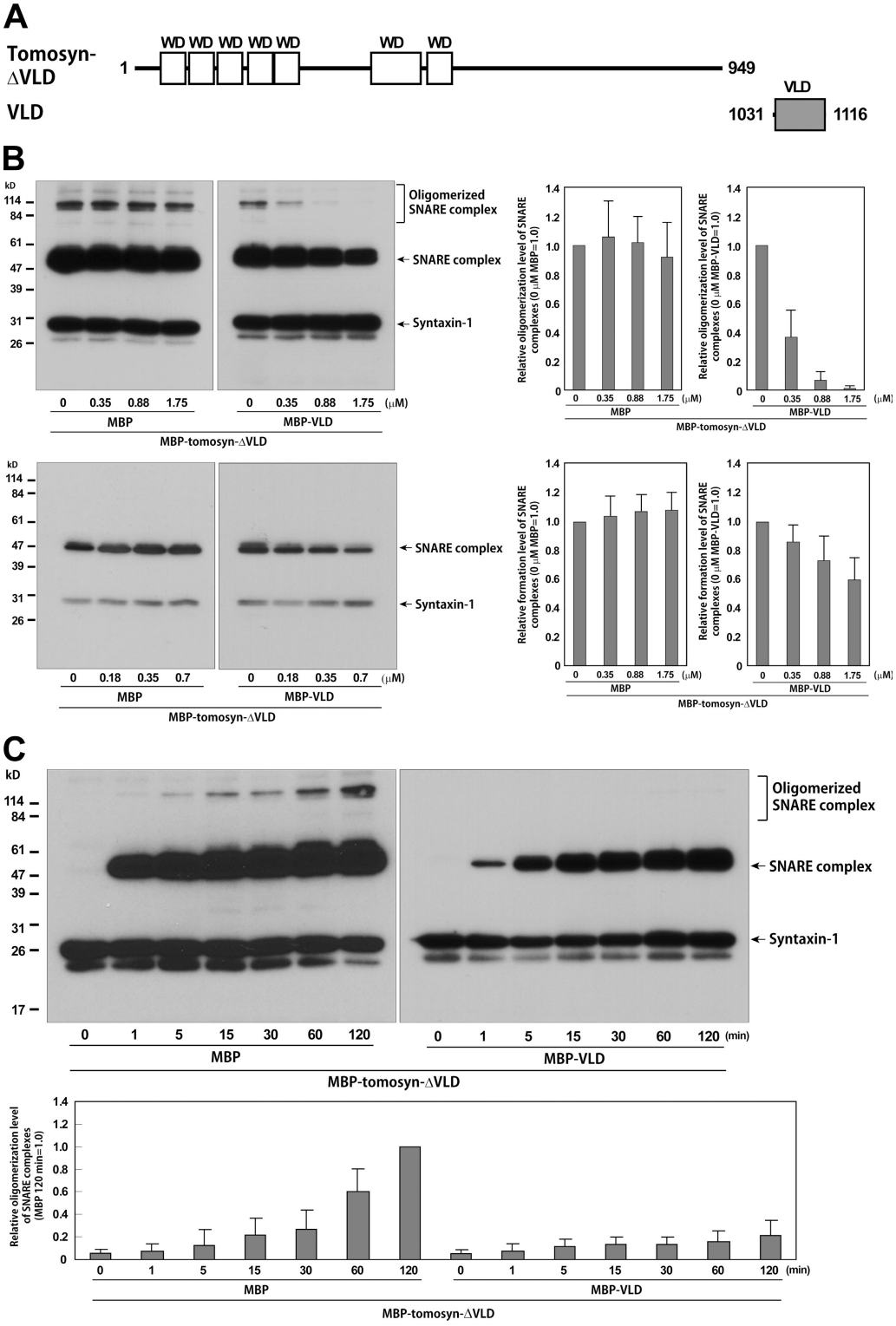

Figure 6. **Regulation of the N-terminal WD-40 repeat domain–induced oligomerization of the SNARE complex by the C-terminal VLD.** (A) Molecular structures of tomosyn-ΔVLD and VLD. (B) Dose-dependent inhibitory effect of the VLD on the tomosyn-ΔVLD–induced oligomerization of the SNARE complex through inhibiting formation of the monomeric SNARE complex. Syntaxin-1, SNAP-25, and MBP-tomosyn-ΔVLD were incubated in the presence of the indicated amounts of MBP or MBP-VLD for 12 h. Each mixture was further incubated with VAMP-2 for 1 h. The proteins were solubilized in the SDS sample buffer at RT and subjected to SDS-PAGE followed by immunoblotting with anti–syntaxin-1 mAb. (top left) Long exposure of the film to detect the oligomerized SNARE complex. (bottom left) Short exposure of the film to detect the ternary SNARE complex. Quantifications of the relative oligomerization of the SNARE complex and the relative formation of the ternary SNARE complex are shown in the right panels. (C) Time-dependent inhibitory effect of the VLD on tomosyn-ΔVLD–induced oligomerization of the SNARE complex. Syntaxin-1, SNAP-25, and MBP-tomosyn-ΔVLD were incubated in the presence of MBP or MBP-VLD for 12 h. Each mixture was further incubated with VAMP-2 for the indicated periods of time. The proteins were solubilized in the SDS sample buffer at RT and subjected to SDS-PAGE followed by immunoblotting with anti–syntaxin-1 mAb. Quantification of the relative oligomerization of SNARE complex is shown in the bottom panel. The results shown are representative of three independent experiments. (B and C) Error bars represent SD.

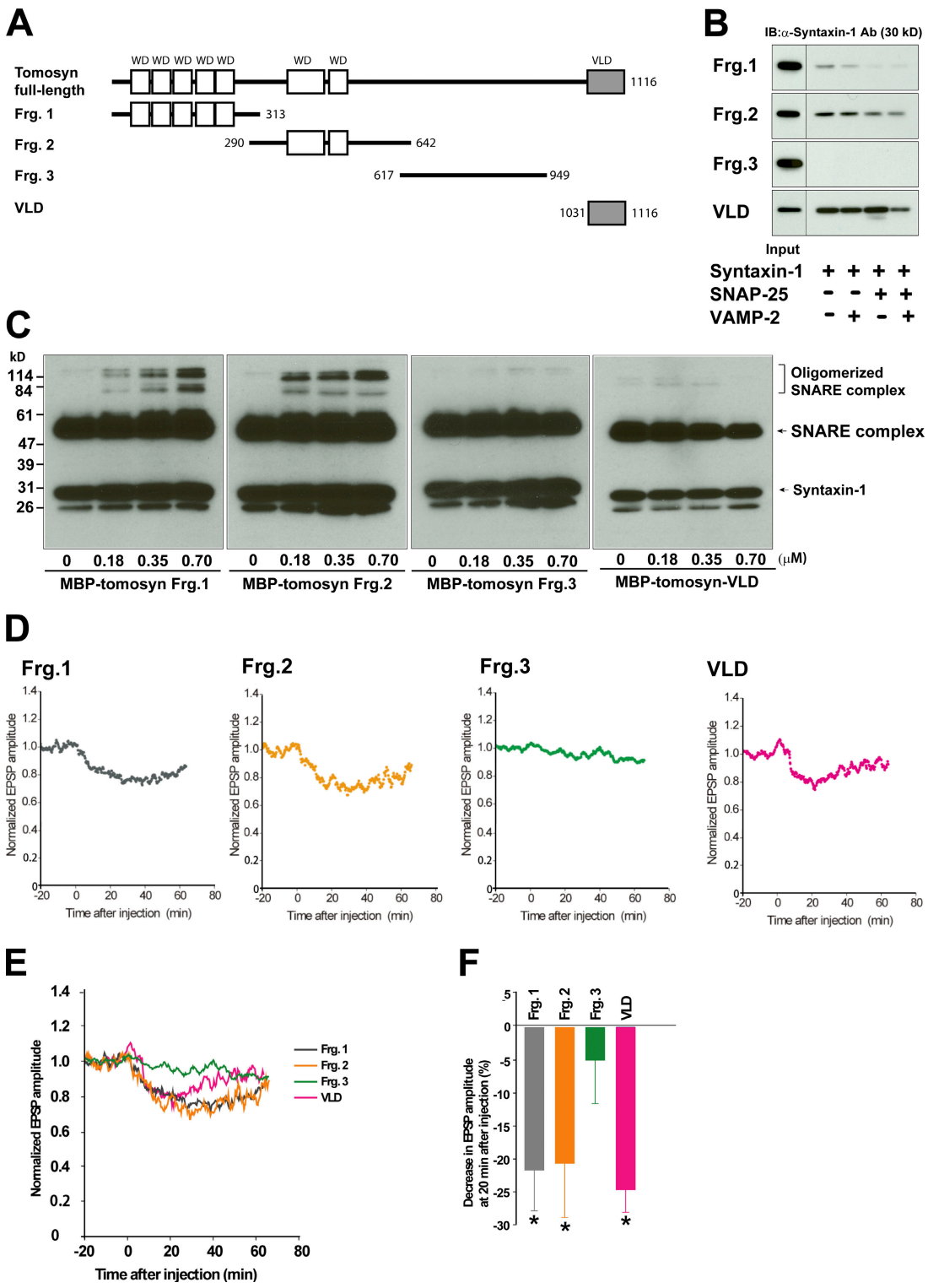

Figure 7. **Functional correlation of the WD-40 repeat domain–enhanced oligomerization of the SNARE complex with inhibition of neurotransmitter release.** (A) Molecular structures of tomosyn fragments. (B) Binding of the tomosyn fragments to syntaxin-1. MBP-fused fragments of tomosyn were immobilized on amylose resin and incubated with recombinant SNARE proteins. The samples were subjected to SDS-PAGE followed by immunoblotting with anti–syntaxin-1 mAb. (C) The tomosyn fragments responsible for the oligomerization of the SNARE complex. The SNARE proteins were reacted in the presence of various amounts of the tomosyn fragment, and samples were solubilized in the SDS sample buffer at RT and subjected to SDS-PAGE followed by immunoblotting with anti–syntaxin-1 mAb. (D) Inhibitory effects of the truncated forms of the WD-40 repeat domain on synaptic transmission between SCG neurons. The MBP-tomosyn fragment was injected into the presynaptic neurons at t = 0 (100 μM in the pipette). EPSP amplitudes measured every 10 s were normalized and averaged (n = 4–9). The mean values smoothed by an eight-point moving average algorithm are plotted. (E) Smoothed mean values shown in D were plotted with lines. (F) Decrease in EPSP amplitudes induced by various MBP-tomosyn fragments are shown in graphs in D. Each bar shows the smoothed mean values of the EPSP amplitudes at 20 min after injection. *, $P < 0.01$, unpaired t test; Frg. 3 injection versus Frg. 1, Frg. 2, or VLD injection. Error bars represent SEM.

Frg. 2–injected neurons suggests that tomosyn-enhanced oligomerization of the SNARE complex potently inhibits neurotransmitter release.

Discussion

In this study, we demonstrated that tomosyn regulates the oligomerization of the SNARE complex and inhibits SNARE-dependent neurotransmitter release. We reconstituted tomosyn-induced oligomerization of the SNARE complex in vitro and showed that the WD-40 repeat domain of tomosyn has an intrinsic ability to catalyze the oligomerization of the SNARE complex. It was previously reported that the C-terminal VLD of tomosyn acts as a SNARE domain competing with VAMP-2 and thereby inhibiting the formation of the SNARE complex (Yokoyama et al., 1999; Pobbati et al., 2004). Consistent with these studies, our in vitro assay showed that the C-terminal VLD of tomosyn inhibits the formation of the SNARE complex. Therefore, we concluded that tomosyn potently inhibits SNARE-dependent synaptic vesicle fusion via both N-terminal WD-40 repeat domain–catalyzed oligomerization of the SNARE complex and C-terminal VLD-based competitive inhibition of SNARE complex formation.

Synaptic efficacy at mossy fiber synapses was enhanced in tomosyn-deficient mice, suggesting that tomosyn inhibits synaptic transmission in normal animals, most likely through regulation of the oligomerization of the SNARE complex. We also demonstrated that PPF was significantly smaller in tomosyn-deficient mice than in littermate wild-type mice. PPF is a physiological measure of the probability of neurotransmitter release from the presynaptic terminal; PPF increases when the probability is decreased but decreases when the probability is increased (Manabe et al., 1993). Thus, the enhanced synaptic efficacy in the input–output relationship in tomosyn-deficient mice is most probably caused by increased probability of neurotransmitter release. Interestingly, there was no difference in the magnitude of mossy fiber LTP measured 50–60 min after tetanic stimulation, whereas short-term potentiation observed for ∼20 min after tetanic stimulation in tomosyn-deficient mice is smaller than that in littermate wild-type mice. These findings indicate that mossy fiber LTP is composed of at least two phases, and only the earlier potentiation is associated with tomosyn-mediated regulation of transmitter release, whereas expression of the later phase of LTP is not mediated by tomosyn. Because basal probability of neurotransmitter release is apparently different between wild-type and tomosyn-deficient mice but the magnitude of LTP at the late phase is not, the expression of mossy fiber LTP is likely to be independent of the initial probability of neurotransmitter release. It has been reported that mossy fiber LTP is mediated by cAMP and PKA (Weisskopf et al., 1994). In this study, the authors found that forskolin, an activator of adenylate cyclase, and membrane-permeable cAMP analogues potentiate mossy fiber EPSPs via the same mechanism underlying mossy fiber LTP induced by tetanic stimulation of mossy fibers; after potentiation by the application of these drugs, no long-lasting potentiation was induced by tetanic stimulation. However, short-term potentiation could still be observed after tetanic stimulation for ∼20–30 min, and this resembled the short-term potentiation that is absent in the tomosyn-deficient mice. Thus, mossy fiber LTP is quite likely to be mediated by two different mechanisms, one of which is dependent on tomosyn and short lasting and the other of which is independent of tomosyn and long lasting.

The activity of the WD-40 repeat domain to catalyze the oligomerization of the SNARE complex was repressed by the C-terminal VLD, suggesting that the catalytic activity of the WD-40 repeat domain competes with C-terminal VLD-based inhibition of SNARE complex formation. Therefore, it is plausible that these two inhibitory actions of tomosyn against the SNARE complexes are properly balanced in vivo. Indeed, we showed that PKA is one possible regulator of this balance. We previously reported that PKA phosphorylates tomosyn, resulting in decreased affinity of the C-terminal VLD for syntaxin-1 (Baba et al., 2005). The PKA-catalyzed phosphorylation of tomosyn increases the fusion-competent readily releasable pool of synaptic vesicles and thereby enhances neurotransmitter release in SCG neurons. In this study, we demonstrated that the PKA-phosphorylated form of tomosyn enhances the oligomerization of the SNARE complex more efficiently than the nonphosphorylated form, indicating that PKA regulates the activity of the WD-40 repeats domain to enhance the oligomerization of the SNARE complex and inhibits neurotransmitter release. The present results are apparently inconsistent with our previous results, but the reason for this inconsistency is unknown. However, the PKA-catalyzed phosphorylation of tomosyn may be more important for balancing the activities of the WD-40 repeat domain and the C-terminal VLD than for altering the affinity of the C-terminal VLD for syntaxin-1. We previously showed that the major phosphorylation site of tomosyn, serine 724, is located at the linker region between the N-terminal WD-40 repeat domain and the C-terminal VLD (Baba et al., 2005). The linker region may act as an intramolecular switch for tomosyn by balancing its two inhibitory effects on SNARE function.

The WD-40 repeat domain of tomosyn shares similarity to the *Drosophila* tumor suppressor D-Lgl, its mammalian homologues M-Lgl1 and M-Lgl2, and the yeast proteins Sro7p and Sro77p, which play important roles in polarized exocytosis by regulating SNARE function on the plasma membrane in *Drosophila* neuroblasts, mammalian epithelial cells, and yeast, respectively (Wirtz-Peitz and Knoblich, 2006). A recent structural study of Sro7 suggested that the N-terminal WD-40 repeat domain of Sro7 interacts with Sec9, a yeast counterpart of SNAP-25, and that this interaction inhibits the formation of the monomeric SNARE complexes (Hattendorf et al., 2007). These results are inconsistent with our present finding that the interaction of the N-terminal WD-40 repeat domain of tomosyn with SNAP-25 did not inhibit the formation of the monomeric SNARE complexes. However, it remains unknown whether the WD-40 repeat domain of Sro7 catalyzes the oligomerization of the SNARE complex as tomosyn does. Further studies of the WD-40 repeat domains of M-Lgl1, M-Lgl2, Sro7, and Sro77 will be needed to understand the conserved role of Lgl family proteins in the regulation of SNARE function.

Materials and methods

Recombinant proteins

Expression vectors for full-length rat medium-sized tomosyn (1–1,116 aa) and tomosyn-ΔVLD (1–949 aa) were constructed in pFastBac1-MBP using standard molecular biology methods. The pFastBac1-MBP vector was constructed from a baculovirus transfer vector, pFastBac1 (Invitrogen), to express a fusion protein with N-terminal MBP (Yasumi et al., 2005). MBP-fused tomosyn and tomosyn-ΔVLD were expressed in Sf21 cells and purified with amylose resin in accordance with the manufacturer's manual. A cDNA encoding the VLD domain (1,031–1,116 aa) of rat medium-sized tomosyn was subcloned into the pMAL-C2 vector (New England Biolabs, Inc.) to express a fusion protein with N-terminal MBP in bacteria. MBP-VLD was expressed in *E. coli* and purified with amylose resin. For the expression of GST-fused syntaxin-1 (GST–syntaxin-1), GST-fused SNAP-25 (GST–SNAP-25), and GST-fused VAMP-2 (GST–VAMP-2), cDNAs encoding the cytoplasmic domain of syntaxin-1 (1–265 aa), full-length SNAP-25 (1–206 aa), and the cytoplasmic domain of VAMP-2 (1–94 aa) were subcloned into pGEX vectors (GE Healthcare). GST–syntaxin-1, GST–SNAP-25, and GS–VAMP-2 were expressed in *E. coli* and purified with glutathione–Sepharose 4B (GE Healthcare) in accordance with the manufacturer's manual. To cut off the GST tags, GST–SNAP-25 was digested with PreScission protease (GE Healthcare), and GST–syntaxin-1 and GST–VAMP-2 were digested with thrombin. The GST tag and PreScission protease in SNAP-25 were removed by glutathione–Sepharose 4B. The GST tags and thrombin in syntaxin-1 and VAMP-2 were removed by glutathione–Sepharose 4B and benzamidine Sepharose, respectively. Syntaxin-1 and VAMP-2 were further purified using Mono-Q (GE Healthcare) and Mono-S columns (GE Healthcare), respectively, as previously described (Fasshauer et al., 1997).

Abs

An antitomosyn pAb was prepared as described previously (Fujita et al., 1998). Anti–syntaxin-1 mAb (10H5) was provided by M. Takahashi (Kitasato University, Kanagawa, Japan). Anti–syntaxin-1 mAb, anti–VAMP-2 mAb (Wako Chemicals USA, Inc.), anti–SNAP-25 mAb (SMI81; Abcam), anti–SNAP-25 mAb (Millipore), anticomplexin pAb (Synaptic Systems GmbH), and anti-MBP pAb (New England Biolabs, Inc.) were purchased from commercial sources. Alexa Fluor–conjugated secondary Abs (Invitrogen) were used to detect primary Abs in immunofluorescence microscopy of brain sections.

Electrophysiology

Male mutant mice and their littermates (6–12 wk old) were used. Hippocampal slices (400-µm thick) were cut with a tissue slicer (Vibratome) and placed in a humidified interface-type holding chamber for at least 1 h. A single slice was transferred to the recording chamber and submerged in a continuously perfusing medium that had been saturated with 95% O_2/5% CO_2. The medium contained 119 mM NaCl, 2.5 mM KCl, 1.3 mM $MgSO_4$, 2.5 mM $CaCl_2$, 1 mM NaH_2PO_4, 26.2 mM $NaHCO_3$, and 11 mM glucose. All experiments were conducted at 25–26°C. Electrical stimuli were delivered through a tungsten bipolar electrode inserted into the stratum granulosum of the dentate gyrus, and the resulting field EPSPs were recorded from the stratum lucidum in the CA3 region with a glass microelectrode filled with 3 M NaCl (1–2 MΩ). PPF of excitatory synaptic transmission was induced by stimulating afferent fibers at short intervals of 30, 50, 100, 300, and 500 ms. LTP of excitatory synaptic transmission was induced in the presence of 50 µM D-APV, an *N*-methyl-D-aspartate receptor antagonist, by applying tetanic stimulation (100 Hz for 1 s) to the mossy fibers. All experiments were performed in a blind fashion. The statistical significance of differences between the genotypes was determined by two-tailed *t* tests.

Glycerol gradient ultracentrifugation of the detergent extracts of mouse cerebral cortex

The detergent extracts of 500 µl of mouse cerebra (1.25 mg of protein) were layered onto 10.5-ml linear 10–40% glycerol gradients in buffer A (20 mM Tris/HCl, pH 7.5, 150 mM NaCl, 5 mM $MgCl_2$, 1 mM EDTA, 1 mM DTT, 10 µM α-phenylmethanesulfonyl fluoride hydrochloride, 10 µg/ml leupeptin, 10 µg/ml aprotinin, and 0.5% NP-40) and subjected to centrifugation at 207,000 *g* for 18 h. Fractions of 1 ml were collected.

Immunohistochemistry

Adult mice were deeply anesthetized by ether and perfused with freshly prepared 2% paraformaldehyde in PBS for 15 min. Brains were dissected out and cut with a razor into several 2-mm-thick coronal sections, which were soaked with the same fixative at 4°C for 2 h. For cryoprotection, sections were placed into 20% sucrose solution for 2 h and 25% sucrose solution overnight. The sections were frozen using liquid nitrogen. Serial 8-µm-thick sections were cut in a cryostat. Each sample was incubated with antitomosyn pAb and anti–SNAP-25 mAb (SMI81) followed by incubation with secondary Alexa Fluor–conjugated secondary Abs. After being washed with PBS, they were embedded and viewed using a confocal laser-scanning microscope (LSM 510-V3.2; Carl Zeiss, Inc.) with a 20 or 40× objective lens. Collected data were exported as 8-bit TIFF files and processed using Photoshop (version 7.0; Adobe).

Electron microscopy

The sample was mixed with an equal volume of glycerol and sprayed on freshly cleaved pieces of mica according to a previously described method (Tyler and Branton, 1980). After drying under 10^{-6} mbar for 15 min, each sample was rotary shadowed with platinum carbon at a shadowing angle of ~5°. Shadowed films were floated on water, picked up onto Formvar-coated grids, and observed in an electron microscope (JEM-1010HC; JEOL) at an accelerating voltage of 100 kV.

Assay for the oligomerization of the SNARE complex

Recombinant syntaxin-1, SNAP-25, VAMP-2, and complexin-2 were purified as GST-fusion proteins and cleaved with thrombin to remove GST. 1 µM syntaxin-1, 1 µM SNAP-25, and 0.1 µM MBP-tomosyn were incubated under reducing conditions (1 mM DTT) at 4°C for 12 h. The mixture was further incubated with 1 µM VAMP-2 at 25°C for 1 h. The reaction was terminated by addition of the SDS sample buffer to give final concentrations of 60 mM Tris/HCl, pH 6.8, 75 mM DTT, 20 mM EDTA, 5% glycerol, and 2% SDS and was further incubated at RT or 100°C for 5 min. Each sample was subjected to SDS-PAGE followed by immunoblotting with anti–syntaxin-1 mAb.

Isolation of the lipid raft fraction

The crude synaptic membrane (CSM) fraction was isolated from 12 mouse brains as described previously (Mizoguchi et al., 1989), and the lipid raft fraction was separated from the CSM fraction as described previously (Vetrivel et al., 2004). In brief, 2 mg of the CSM fraction was resuspended in TNE buffer (20 mM Tris/HCl, pH 7.5, 150 mM NaCl, and 1 mM EDTA) containing 0.5% Lubrol WX at 4°C for 30 min, and 40% sucrose was added. A discontinuous sucrose gradient was made by layering 30% sucrose (3 ml), 25% sucrose (3 ml), and 5% sucrose (3 ml) onto the sample (2 ml), and the gradient was subjected to ultracentrifugation at 201,800 *g* for 2 h at 4°C. 11 1-ml fractions were collected from the top of the gradient, and an equal volume of each fraction was analyzed by immunoblotting. The lipid raft fraction was determined by immunoblotting for flotillin-2, a lipid raft–associated protein.

Assay for the binding of syntaxin-1 or SNAP-25 to tomosyn

Syntaxin-1, SNAP-25, the mixture of syntaxin-1 and SNAP-25, or the mixture of syntaxin-1, SNAP-25, and VAMP-2 was incubated with MBP, MBP-tomosyn-ΔVLD, or MBP-VLD immobilized on 50 µl of amylose beads in 500 µl of buffer B (20 mM Tris/HCl, pH 7.5, 150 mM NaCl, 1 mM EDTA, 1 mM DTT, 5 mM $MgCl_2$, and 0.5% NP-40) at 25°C for 1 h. After the beads had been extensively washed with buffer B, the bound proteins were solubilized in the SDS sample buffer and further incubated at RT or 100°C for 5 min. Each sample was subjected to SDS-PAGE followed by immunoblotting with anti–syntaxin-1 mAb, anti–SNAP-25 mAb, or anti–VAMP-2 mAb. The intensity of the immunoblot band was determined by densitometry.

Culture of SCG neurons

Postnatal day 7 Wistar ST rats were decapitated under diethyl ether anesthesia according to the guidelines of the Physiological Society of Japan. Isolated SCG neurons were maintained in culture for 5–6 wk as described previously (Mochida et al., 1994; Mochida, 1995). In brief, SCGs were dissected, desheathed, and incubated with 0.5 mg/ml collagenase (Worthington Biochemical) in L-15 (Invitrogen) at 37°C for 10 min. After enzyme digestion, semidissociated ganglia were triturated gently through small-pore glass pipettes until a cloudy suspension was observed. After washing by low speed centrifugation at 1,300 rpm for 3 min, the collected cells were plated onto coverslips in plastic dishes (35-mm diameter; approximately one ganglion per dish; Corning) containing a growth medium of 84% Eagle's minimal essential medium (Invitrogen), 10% fetal calf serum (Invitrogen), 5% horse serum (Invitrogen), 1% penicillin/streptomycin (Invitrogen), and 25 ng/ml nerve growth factor (2.5 S; grade II; Alomone Laboratories). The cells were maintained at 37°C in a 95% air and 5% CO_2 humidified incubator, and the medium was changed twice per week.

Synaptic transmission between SCG neurons

EPSP recording and injection of the recombinant proteins were performed as described previously (Mochida et al., 1994, 1996). Electrophysiological data collected using software written by the late L. Tauc (Centre National de la Recherche Scientifique, Gif-sur-Yvette, France) were analyzed with Origin (Microcal Software Inc.). For Fig. 7 D, the peak amplitudes of EPSP were averaged. The resultant values were smoothed by an eight-point moving average algorithm and plotted against recording time with t = 0 indicating the presynaptic injection. For Fig. 7 F, data at 20 min after injection from each group were averaged, and statistical significance was determined by unpaired Student's *t* tests (vs. the Frg. 3–injected group).

Online supplemental material

Fig. S1 shows characterization of the high molecular weight SNARE complex. Fig. S2 shows validation of tomosyn-enhanced oligomerization of the SNARE complex. Fig. S3 shows tomosyn-independent oligomerization of the SNARE complex facilitated by the transmembrane domains of the SNARE proteins. Fig. S4 shows characterization of the tomoysn-enhanced oligomerization of the SNARE complex. Fig. S5 shows the effect of the PKA-catalyzed phosphorylation of tomosyn on the oligomerization of the SNARE complex and binding of SNAP-25 to the WD-40 repeat domain of tomosyn.

This work was supported by Grants-in-Aid for the National Project on Targeted Proteins Research Program (T. Sakisaka), for Scientific Research B (S. Mochida), for Specially Promoted Research (Y. Fujiyoshi), for Scientific Research (T. Manabe), for the Center for the Brain Medical Science, 21st Century Centers of Excellence Program (T. Manabe), and for Cancer Research (Y. Takai) from the Ministry of Education, Culture, Sports, Science and Technology and by grants from the Japan Science and Technology Agency (Y. Fujiyoshi) and the Japan New Energy and Industrial Technology Development Organization (Y. Fujiyoshi).

Submitted: 26 May 2008
Accepted: 12 September 2008

References

Baba, T., T. Sakisaka, S. Mochida, and Y. Takai. 2005. PKA-catalyzed phosphorylation of tomosyn and its implication in Ca^{2+}-dependent exocytosis of neurotransmitter. *J. Cell Biol.* 170:1113–1125.

Bennett, M.K., N. Calakos, and R.H. Scheller. 1992. Syntaxin: a synaptic protein implicated in docking of synaptic vesicles at presynaptic active zones. *Science.* 257:255–259.

Chen, Y.A., and R.H. Scheller. 2001. SNARE-mediated membrane fusion. *Nat. Rev. Mol. Cell Biol.* 2:98–106.

Chen, Y.A., S.J. Scales, S.S. Patel, Y.C. Doung, and R.H. Scheller. 1999. SNARE complex formation is triggered by Ca^{2+} and drives membrane fusion. *Cell.* 97:165–174.

Constable, J.R., M.E. Graham, A. Morgan, and R.D. Burgoyne. 2005. Amisyn regulates exocytosis and fusion pore stability by both syntaxin-dependent and syntaxin-independent mechanisms. *J. Biol. Chem.* 280:31615–31623.

Dai, H., N. Shen, D. Araç, and J.A. Rizo. 2007. A quaternary SNARE-synaptotagmin-Ca2+-phospholipid complex in neurotransmitter release. *J. Mol. Biol.* 367:848–863.

Fasshauer, D., H. Otto, W.K. Eliason, R. Jahn, and A.T. Brünger. 1997. Structural changes are associated with soluble N-ethylmaleimide-sensitive fusion protein attachment protein receptor complex formation. *J. Biol. Chem.* 272:28036–28041.

Fujita, Y., H. Shirataki, T. Sakisaka, T. Asakura, T. Ohya, H. Kotani, S. Yokoyama, H. Nishioka, Y. Matsuura, A. Mizoguchi, et al. 1998. Tomosyn: a syntaxin-1-binding protein that forms a novel complex in the neurotransmitter release process. *Neuron.* 20:905–915.

Gracheva, E.O., A.O. Burdina, A.M. Holgado, M. Berthelot-Grosjean, B.D. Ackley, G. Hadwiger, M.L. Nonet, R.M. Weimer, and J.E. Richmond. 2006. Tomosyn inhibits synaptic vesicle priming in *Caenorhabditis elegans*. *PLoS Biol.* 4:e261.

Hatsuzawa, K., T. Lang, D. Fasshauer, D. Bruns, and R. Jahn. 2003. The R-SNARE motif of tomosyn forms SNARE core complexes with syntaxin 1 and SNAP-25 and down-regulates exocytosis. *J. Biol. Chem.* 278:31159–31166.

Hattendorf, D.A., A. Andreeva, A. Gangar, P.J. Brennwald, and W.I. Weis. 2007. Structure of the yeast polarity protein Sro7 reveals a SNARE regulatory mechanism. *Nature.* 446:567–571.

Hayashi, T., H. McMahon, S. Yamasaki, T. Binz, Y. Hata, T.C. Südhof, and H. Niemann. 1994. Synaptic vesicle membrane fusion complex: action of clostridial neurotoxins on assembly. *EMBO J.* 13:5051–5061.

Hohl, T.M., F. Parlati, C. Wimmer, J.E. Rothman, T.H. Söllner, and H. Engelhardt. 1998. Arrangement of subunits in 20 S particles consisting of NSF, SNAPs, and SNARE complexes. *Mol. Cell.* 2:539–548.

Hu, K., J. Carroll, C. Rickman, and B. Davletov. 2002. Action of complexin on SNARE complex. *J. Biol. Chem.* 277:41652–41656.

Jahn, R., and R.H. Scheller. 2006. SNAREs–engines for membrane fusion. *Nat. Rev. Mol. Cell Biol.* 7:631–643.

Jahn, R., and T.C. Südhof. 1999. Membrane fusion and exocytosis. *Annu. Rev. Biochem.* 68:863–911.

Lehman, K., G. Rossi, J.E. Adamo, and P. Brennwald. 1999. Yeast homologues of tomosyn and lethal giant larvae function in exocytosis and are associated with the plasma membrane SNARE, Sec9. *J. Cell Biol.* 146:125–140.

Ma, H., and S. Mochida. 2007. A cholinergic model synapse to elucidate protein function at presynaptic terminals. *Neurosci. Res.* 57:491–498.

Manabe, T., D.J.A. Wyllie, D.J. Perkel, and R.A. Nicoll. 1993. Modulation of synaptic transmission and long-term potentiation: effects on paired pulse facilitation and EPSC variance in the CA1 region of the hippocampus. *J. Neurophysiol.* 70:1451–1459.

McEwen, J.M., J.M. Madison, M. Dybbs, and J.M. Kaplan. 2006. Antagonistic regulation of synaptic vesicle priming by Tomosyn and UNC-13. *Neuron.* 51:303–315.

Mizoguchi, A., T. Ueda, K. Ikeda, H. Shiku, H. Mizoguti, and Y. Takai. 1989. Localization and subcellular distribution of cellular ras gene products in rat brain. *Brain Res. Mol. Brain Res.* 5:31–44.

Mochida, S. 1995. Role of myosin in neurotransmitter release: functional studies at synapses formed in culture. *J. Physiol. Paris* 89:83–94.

Mochida, S., Y. Nonomura, and H. Kobayashi. 1994. Analysis of the mechanism for acetylcholine release at the synapse formed between rat sympathetic neurons in culture. *Microsc. Res. Tech.* 29:94–102.

Mochida, S., Z.H. Sheng, C. Baker, H. Kobayashi, and W.A. Catterall. 1996. Inhibition of neurotransmission by peptides containing the synaptic protein interaction site of N-type Ca^{2+} channels. *Neuron.* 17:781–788.

Pabst, S., M. Margittai, D. Vainius, R. Langen, R. Jahn, and D. Fasshauer. 2002. Rapid and selective binding to the synaptic SNARE complex suggests a modulatory role of complexins in neuroexocytosis. *J. Biol. Chem.* 277:7838–7848.

Pobbati, A.V., A. Razeto, M. Boddener, S. Becker, and D. Fasshauer. 2004. Structural basis for the inhibitory role of tomosyn in exocytosis. *J. Biol. Chem.* 279:47192–47200.

Puri, N., and P.A. Roche. 2006. Ternary SNARE complexes are enriched in lipid rafts during mast cell exocytosis. *Traffic.* 7:1482–1494.

Rickman, C., K. Hu, J. Carroll, and B. Davletov. 2005. Self-assembly of SNARE fusion proteins into star-shaped oligomers. *Biochem. J.* 388:75–79.

Sakisaka, T., T. Baba, S. Tanaka, G. Izumi, M. Yasumi, and Y. Takai. 2004. Regulation of SNAREs by tomosyn and ROCK : implication in extension and retraction of neurites. *J. Cell Biol.* 166:17–25.

Salaün, C., G.W. Gould, and L.H. Chamberlain. 2005. Lipid raft association of SNARE proteins regulates exocytosis in PC12 cells. *J. Biol. Chem.* 280:19449–19453.

Söllner, T., M.K. Bennett, S.W. Whiteheart, R.H. Scheller, and J.E. Rothman. 1993. A protein assembly-disassembly pathway in vitro that may correspond to sequential steps of synaptic vesicle docking, activation, and fusion. *Cell.* 75:409–418.

Südhof, T.C. 2000. The synaptic vesicle cycle revisited. *Neuron.* 28:317–320.

Sutton, R.B., D. Fasshauer, R. Jahn, and A.T. Brunger. 1998. Crystal structure of a SNARE complex involved in synaptic exocytosis at 2.4 Å resolution. *Nature.* 395:347–353.

Tokumaru, H., K. Umayahara, L.L. Pellegrini, T. Ishizuka, H. Saisu, H. Betz, G.J. Augustine, and T. Abe. 2001. SNARE complex oligomerization by synaphin/complexin is essential for synaptic vesicle exocytosis. *Cell.* 104:421–432.

Trimble, W.S., D.M. Cowan, and R.H. Scheller. 1988. VAMP-1: a synaptic vesicle-associated integral membrane protein. *Proc. Natl. Acad. Sci. USA.* 85:4538–4542.

Tyler, J.M., and D. Branton. 1980. Rotary shadowing of extended molecules dried from glycerol. *J. Ultrastruct. Res.* 71:95–102.

Vetrivel, K.S., H. Cheng, W. Lin, T. Sakurai, T. Li, N. Nukina, P.C. Wong, H. Xu, and G. Thinakaran. 2004. Association of gamma-secretase with lipid rafts in post-Golgi and endosome membranes. *J. Biol. Chem.* 279:44945–44954.

Weber, T., B.V. Zemelman, J.A. McNew, B. Westermann, M. Gmachl, F. Parlati, T.H. Söllner, and J.E. Rothman. 1998. SNAREpins: minimal machinery for membrane fusion. *Cell.* 92:759–772.

Weis, W.I., and R.H. Scheller. 1998. Membrane fusion. SNARE the rod, coil the complex. *Nature.* 395:328–329.

Weisskopf, M.G., P.E. Castillo, R.A. Zalutsky, and R.A. Nicoll. 1994. Mediation of hippocampal mossy fiber long-term potentiation by cyclic AMP. *Science.* 265:1878–1882.

Wirtz-Peitz, F., and J.A. Knoblich. 2006. Lethal giant larvae take on a life of their own. *Trends Cell Biol.* 16:234–241.

Yasumi, M., T. Sakisaka, T. Hoshino, T. Kimura, Y. Sakamoto, T. Yamanaka, S. Ohno, and Y. Takai. 2005. Direct binding of Lgl2 to LGN during mitosis and its requirement for normal cell division. *J. Biol. Chem.* 280:6761–6765.

Yizhar, O., N. Lipstein, S.E. Gladycheva, U. Matti, S.A. Ernst, J. Rettig, E.L. Stuenkel, and U. Ashery. 2007. Multiple functional domains are involved in tomosyn regulation of exocytosis. *J. Neurochem.* 103:604–616.

Yokoyama, S., H. Shirataki, T. Sakisaka, and Y. Takai. 1999. Three splicing variants of tomosyn and identification of their syntaxin-binding region. *Biochem. Biophys. Res. Commun.* 256:218–222.